



One plus Two: Supramolecular Coordination in a Nano-Reactor on Surface

Xuemei Zhang, Yongtao Shen, Shuai Wang, Yuanyuan Guo, Ke Deng, Chen Wang & Qingdao Zeng

National Center for Nanoscience and Technology (NCNST), Beijing 100190, P. R. China.

Received
7 July 2012

Accepted
17 September 2012

Published
17 October 2012

Correspondence and requests for materials should be addressed to Q.Z. (zengqd@nanocr.cn), C.W. (wangch@nanocr.cn) or K.D. (kdeng@nanocr.cn)

The supramolecular coordination of zinc (II) phthalocyanine (Zn-Pc) with V-shaped bi-pyridine in a nano-reactor is probed by scanning tunneling microscopy (STM) at liquid/solid interface. Combined with density functional theory (DFT) calculations, our STM results show that the V-shaped bi-pyridine and Zn-Pc can generate stable “odd-even” patterned architectures in the TCDB network through a two-step coordination process. Moreover, great changes for the size and the shape of the host cavity have happened during the coordination process. In general, the whole coordination process is regulated by the synergies of ligand and template. To the best of our knowledge, this is the first work on imaging of supramolecular coordination in a nano-reactor. Such a template-regulated supramolecular interconversion opens a new avenue towards the crystal engineering and design as well as the generation of controllable nano-patterns.

Crystal engineering and design of solid-state architecture through self-assembly have been gaining much attention in recent years^{1–4}. Such an approach can lead to the formation of non-covalent bonds ‘at will’ to facilitate the synthesis of large and well-defined molecular architectures and to promote reversible encapsulation^{5–7}. In particular, the metal coordination has been represented as a successful strategy for engineering the functional materials, for this method offers the flexibility of using basic molecular building blocks and a cementing metal atom to construct extended coordination networks^{8,9}. One of the most studied systems is displayed by metal atom bridged-porphyrins or phthalocyanine (Pcs), which is also a typical heme unit in both intact heme proteins and model heme systems^{10–13}. Alternatively, the combination of surface-confined chemistry and scanning tunneling microscopy (STM) techniques allows direct insights into supramolecular coordination at the sub-molecular resolution level^{14,15}. Recent studies have demonstrated that pyridines (Pys) are also one of the promising candidates for molecular architecture, due to the strong metal-ligand interaction between nitrogen atom in Py and the metal atoms^{16–19}. These studies mainly discussed the metal coordination in open nano-scaled environments, that is, the ligand can mobilize freely so as to form varieties of stable assemblies. In contrast, the molecular species in confined space can strongly modify the interaction pathways compared to homogenous and bulk conditions²⁰. However, to the best of our knowledge, there is no report on this kind of cavity confined coordination on surface.

Herein, utilizing the intermolecular H-bonded network of 1,3,5-tris(10-carboxydecyloxy) benzene (TCDB) as a template, we have probed the supramolecular coordination of zinc (II) phthalocyanine (Zn-Pc) with 1,3-di(4-pyridyl)propane (dipy-pra) (Figure 1) in the nano-template through the STM technique at liquid/solid interface, and what we focus on are the role of the template in the supramolecular coordination process and the supramolecular coordination effects on the host-guest network.

Results

TCDB can form two-dimensional networks on HOPG with well-defined nano-scaled pores which can immobilize organic molecules such as the coronene and phthalocyanine as well as other macrocycles²¹, thus it can also be used as a nano-reactor where photo-isomerization of NN-Macrocycles has been studied^{22,23}. Furthermore, the size and geometry of the TCDB network cavities could be modulated to appreciably enhance the adsorption efficiency of the guest molecules, just because of the three flexible alkyl chains and the intermolecular hydrogen bonds^{24,25}.

Prior to investigating the template effect on supramolecular coordination, we firstly immobilize the Zn-Pc into the nanopores of TCDB. Figure 2a shows the well-ordered assembled structure of TCDB/Zn-Pc, from which these two individual molecules can be clearly resolved. Two TCDB molecules fabricate a tetragonal cavity by the alkyl

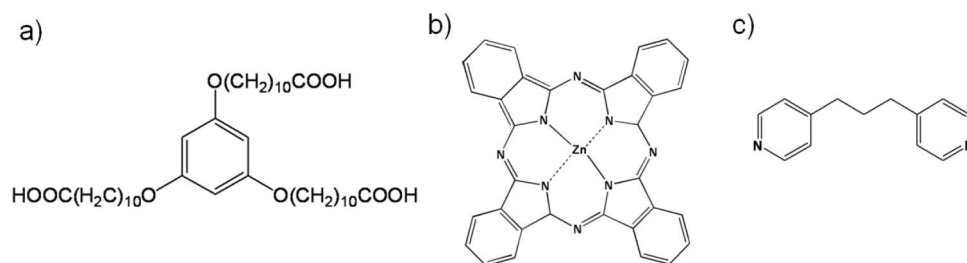


Figure 1 | Chemical structures of (a) TCDB; (b) Zn-Pc; and (c) dipy-pra.

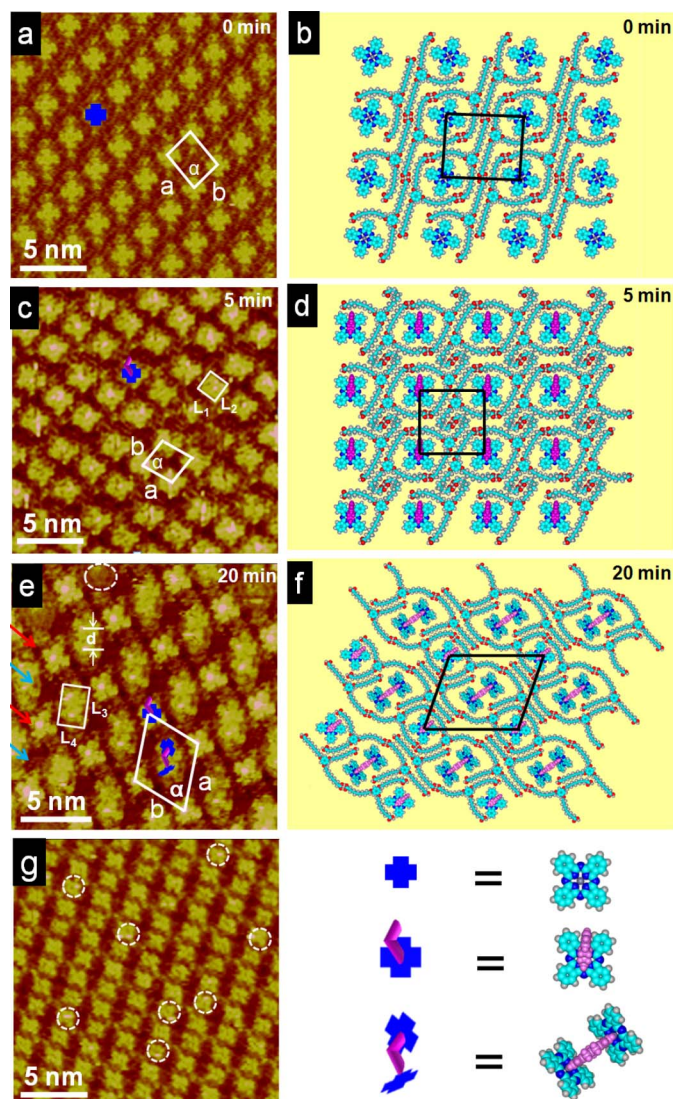


Figure 2 | STM images and molecular models. (a) Assembled structure of TCDB/Zn-Pc. (b) Suggested molecular model for the observed area in (a). (c) Assembled structure of TCDB/Zn-Pc after the dipy-pra molecule was added for 5 minutes. (d) A tentative model for the observed area in (c), the pink part represents the dipy-pra molecules. (e) Assembled structure of TCDB/Zn-Pc after the dipy-pra molecule was added for 20 minutes. (f) The suggested molecular model corresponds to the scanned area in (e), the pink part represents the dipy-pra molecule. (g) Assembled structure of TCDB/Zn-Pc/dipy-pra upon the addition of the HTf solution. Tunneling parameters: $I_{\text{set}} = 299.1$ pA, $V_{\text{bias}} = 600$ mV.

chains connected by intermolecular hydrogen bonds, and one X-shaped Zn-Pc molecule is entrapped into the tetragonal cavity ($m_1 \times n_1 = 2.0$ nm \times 1.8 nm).

To further gain insight into how the Zn-Pc molecules interact with the dipy-pra molecule in TCDB networks, initial growth of supra-molecular complex was accomplished. For the system of TCDB/Zn-Pc/dipy-pra, Figures 2c and 2e display two different assembled structures. At first, when introducing the dipy-pra solution, bright “ \perp ”-shaped complex 1 can be clearly observed 5 minutes later (Figure 2c). Larger than the size of the Zn-Pc molecule ((1.2 ± 0.1) nm \times (1.2 ± 0.1) nm), the size of complex 1 in the cavities is measured to be $L_1 \times L_2 = (1.6 \pm 0.1)$ nm \times (1.6 ± 0.1) nm, showing that the complex 1 is a newly formed compound. As marked in Figure 2c, the bright spot upset (drawn in “ \wedge ”-shaped red characteristic) can be ascribed to the dipy-pra molecule, while the lower layer (drawn in X-shaped blue characteristic) should be the Zn-Pc molecule. Unlike the well-defined TCDB/Zn-Pc system, the co-assembled structure of TCDB/complex 1 seems unstable and shows a random arrangement, which may result from the irregular rotation of the dipy-pra in the complex 1. Interestingly, 20 minutes later, “odd-even” arranged architecture appears (Figure 2e). Along the red arrows, every cavity of TCDB immobilizes one bright “ \perp ”-shaped molecule which should be attributed to the complex 1, forming the “odd” pattern. While along the blue arrows, every cavity is filled with one bright “ \wedge ”-shaped complex 2, presenting the “even” patterned organization. From Figure 2e, the size of this new complex is measured to be $L_3 \times L_4 = (2.9 \pm 0.1)$ nm \times (1.7 ± 0.1) nm, and two X-shaped Zn-Pc molecules can be clearly resolved in another newly formed individual molecule. Besides, the distance (d) between the centers of two Zn-Pc molecules in the complex 2 is in accordance with the length of one dipy-pra molecule (1.2 ± 0.1 nm), which indicates that the “ \wedge ”-shaped complex 2 should be formed by two Zn-Pc molecules bridging with one dipy-pra molecule. A unit cell (the unit cell parameters: $a = 4.8 \pm 0.1$ nm, $b = 4.0 \pm 0.1$ nm and $\alpha = 72 \pm 2.0^\circ$), consisting of one complex 1 and one complex 2, can be seen in this kind of co-assembled structure (Figure 2f). Moreover, some defects appear in the “even” pattern. As shown in Figure 2g, interestingly, upon addition of some 1-phenyloctane solution containing trifluoromethanesulfonic acid (HTf), this kind of “odd-even”

Table 1 | Experimental (Expt.) and calculated (Cal.) lattice parameters for the 2D networks

		unit cell parameters		
		a (nm)	b (nm)	α ($^\circ$)
TCDB/Zn-Pc	Expt.	3.1 ± 0.1	2.2 ± 0.1	87 ± 1.0
	Cal.	3.10	2.44	87.5
TCDB/complex 1	Expt.	2.8 ± 0.1	2.4 ± 0.1	87 ± 2.0
	Cal.	2.80	2.60	90.0
TCDB/complex 2	Expt.	4.8 ± 0.1	4.0 ± 0.1	72 ± 2.0
	Cal.	4.85	4.05	72.0



Table 2 | Total energies (E_{total}) for the 2D networks. The total energy includes the interaction between adsorbates (TCDB network and the guest molecules), and the interaction between the adsorbates and graphite. Here, the guest molecules are Zn-Pc, complex **1** and complex **2**.

	TCDB/Zn-Pc	TCDB/complex 1	TCDB/complex 2
E_{total}	$-223.34 \text{ kcal mol}^{-1}$	$-218.20 \text{ kcal mol}^{-1}$	$-406.06 \text{ kcal mol}^{-1}$

alternately pattern disappears and the original highly ordered TCDB/Zn-Pc and TCDB/complex **1** (indicated by the dotted circles) system can be regenerated. Due to the salinization of bi-pyridines by HTf²⁶, the interaction between the Zn-Pc and the dipy-pira molecule becomes weaker, and the former coordinated Zn-Pc or dipy-pira molecule is released from the supramolecular complexes **2**.

Discussion

Based on these observed phenomena and combined with the density functional theory (DFT) calculations (see table 1 and table 2), we suggest that a two-step process may happen during the coordination of Zn-Pc with dipy-pira in the network of the TCDB molecule (Figure 3). Firstly, the Zn-Pc molecule in the cavity connects with one dipy-pira molecule, generating the bright “ \perp ”-shaped complex **1**. At the same time, through stretching of the alkyl chains, the TCDB network will adjust its cavity size ($m_2 \times n_2 = 2.1 \text{ nm} \times 1.7 \text{ nm}$) so as to immobilize this new formed complex suitably. To compare the thermal dynamic stability of TCDB/complex **1** and TCDB/complex **2**, we have calculated the total energy of the system (see Table 2). Here, the more negative energy means the system is more stable. As described in Table 2, the total energy of TCDB/complex **1** and TCDB/complex **2** is $-218.20 \text{ kcal mol}^{-1}$ and $-406.06 \text{ kcal mol}^{-1}$, respectively, which indicates the structural transformation from TCDB/complex **1** to TCDB/complex **2** is energetically preferable. Secondly, due to the existence of another non-coordinated pyridine of the dipy-pira molecule, the complex **1** in the nanopores is apt to adsorb another Zn-Pc molecule from solution. Once another Zn-Pc molecule in solution is caught, the alkyl chains of the TCDB molecules should be regulated and extend simultaneously to fabricate much larger cavities. As a result, two kinds of cavities (A and B)

are formed. The size of comparatively larger A-type cavity and the smaller B-type cavity is $m_A = 3.4 \text{ nm}$, $n_A = 1.7 \text{ nm}$ and $m_B = 2.1 \text{ nm}$, $n_B = 1.7 \text{ nm}$, respectively. Because of the confinement of the cavity, only A-typed cavity can accommodate two Zn-Pc molecules, that is to say, only cavity A can be used as a reactor for formation of the bright “ \perp ”-shaped complex **2**, whereas the complex **1** in B-typed cavity can not coordinate with another Zn-Pc molecule any more. Moreover, not every complex **1** in A-typed cavity can catch the Zn-Pc molecule from solution, thus the non-coordinated complex **1** can not be well immobilized in the larger cavity A and easily escapes from the TCDB network, resulting in some defects in the “even” pattern.

However, in solution, one Zn-Pc molecule can only coordinate with one dipy-pira molecule through the zinc-pyridine interactions. Beside, displaying in Figure 4, when we perform the coordination of Zn-Pc with dipy-pira (without TCDB) or add the mixed solution of Zn-Pc/dipy-pira into the TCDB networks, we can not directly observe the “odd-even” alternate arrangement²⁷, which well demonstrates that the two-step supramolecular coordination process possibly happens on graphite surface.

On the other hand, the size and shape of the TCDB cavity have been tuned during the coordination process, and such transformation, in turn, affects the coordination process. Especially, the formation of two types of cavities plays a vital role in the generation of the “ \perp ”-shaped complex **2**, which leads to the newly alternate architecture.

In summary, on graphite surface, we have presented an interesting assembled structure initiated by the supramolecular coordination of Zn-Pc with V-shaped bi-pyridine in a flexible molecule template. STM results show that “ \perp ”-shaped complex **1** and “ \perp ”-shaped complex **2** are successively produced in the TCDB network, and an interesting “odd-even” patterned architecture is generated through a two-step coordination process. In order to well accommodate the supramolecular complexes, dramatic changes for the size and the shape of the host cavity can be observed during the coordination process. Based on the DFT calculation, we can see this kind of coordination process is regulated by synergies of ligand and template. Besides, upon the addition of HTf, we found the alternately arranged pattern can be transformed into the original highly ordered assembly. We believe that such a template-regulated supramolecular inter-conversion will open new avenues towards the crystal engineering and design as well as the generation of controlled nanopatterned architectures.

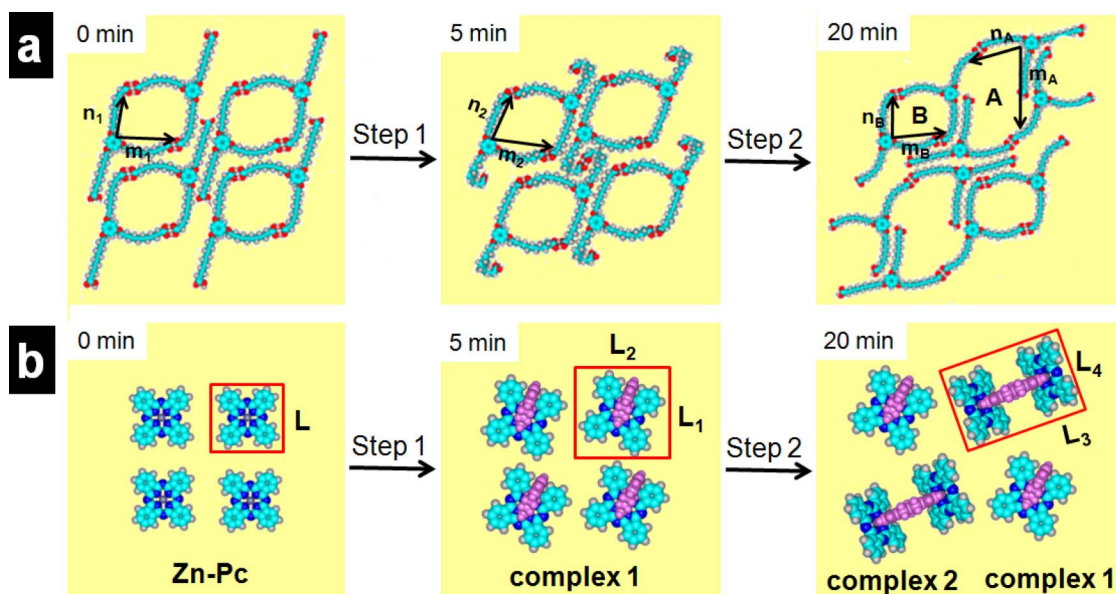


Figure 3 | (a) The molecular models for the transformation of the TCDB networks. (b) Presentation for the formations of complex **1** and complex **2** from the Zn-Pc molecule. The pink parts in complex **1** and complex **2** symbolize the dipy-pira molecules.

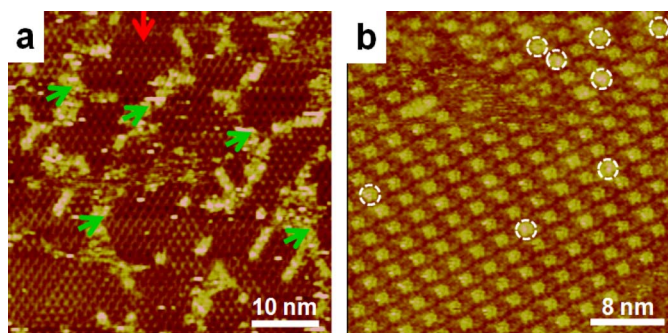


Figure 4 | (a) Self-assembled structure of Zn-Pc/dipy-pra (without template). The part indicated by the red arrow is the assembled structure of Zn-Pc molecules, and the area (indicated by the green arrows) shows the assembled structure of Zn-Pc/dipy-pra. Without TCDB, the assembled structure of Zn-Pc/dipy-pra is disordered, and the "odd-even" nanopattern can not be observed under this case. (b) The coassembled structure of TCDB/Zn-Pc + dipy-pra (upon addition of mixed solution of Zn-Pc and dipy-pra into the TCDB networks). The dotted circles symbolize the few coordinated molecules which can be ascribed to the supramolecular complex 1. Tunnelling parameters are: $I_{set} = 300.0$ pA, $V_{bias} = 600.0$ mV. These two images show that the TCDB networks regulated the formation of complex 2.

Methods

Materials. TCDB was synthesized according to the reported procedures²¹. Zn-Pc, dipy-pra and 1-phenyloctane were purchased from TCI Company, HTf was bought from Aldrich Company, and all these materials were used without any purification.

Sample preparation. TCDB, Zn-Pc, and dipy-pra were dissolved in 1-phenyloctane with concentration less than 10^{-4} M. Firstly, a droplet (0.4 μ L) of the 1-phenyl octane solution containing TCDB, Zn-Pc, and a TCDB/ Zn-Pc mixture (1:1) was deposited respectively onto a freshly cleaved surface (5 mm \times 5 mm) of highly oriented pyrolytic graphite (HOPG, grade ZYB, Advanced Ceramics Inc., Cleveland, USA). A few minutes later, the sample was studied by STM. Secondly, a droplet (0.4 μ L) of 1-phenyloctane solution containing dipy-pra ($<10^{-4}$ M) was added into the studied sample. After 5 minutes and 20 minutes later, the STM investigation was performed. Thirdly, a drop of 1-phenyloctane solution containing HTf ($<10^{-4}$ M) was applied onto the sample. In the end, after 20 minutes, the STM investigation was performed.

STM investigation. The STM measurements were performed on a Nano IIIa scanning probe microscope system (Bruker, USA) under ambient conditions. All STM images presented were recorded in constant current mode using a mechanically cut Pt/Ir (80/20) tip. The thermal drift was corrected using the underlying graphite lattice as a reference. The latter lattice was visualized by lowering the bias voltage to 60 mV and raising the current to 300 pA. And the "error values" on the lattice parameters are obtained by the statistical method.

Computational details. The theoretical calculation was performed using density functional theory (DFT) provided by the DMol3 code^{28–30}. The Perdew and Wang parameterization³¹ of the local exchange correlation energy are applied in the local spin density approximation (LSDA) to describe exchange and correlation. We expanded the all-electron spin-unrestricted Kohn-Sham wave functions in a local atomic orbital basis. In such double-numerical basis set polarization was described. All calculations were all-electron ones, and performed with the Extra-Fine mesh. Self-consistent field procedure was done with a convergence criterion of 10^{-5} a.u. on the energy and electron density.

- Barth, J. V., Costantini, G. & Kern, K. Engineering atomic and molecular nanostructures at surfaces. *Nature* **437**, 671–679 (2005).
- Noveron, J. C. *et al.* Engineering the structure and magnetic properties of crystalline solids via the metal-directed self-assembly of a versatile molecular building unit. *J. Am. Chem. Soc.* **124**, 6613–6625 (2002).
- MacGillivray, L. R., Reid, J. L. & Ripmeester, J. A. Supramolecular control of reactivity in the solid state using linear molecular templates. *J. Am. Chem. Soc.* **122**, 7817–7818 (2000).
- Furukawa, S. & De Feyter, S. Two-dimensional crystal engineering at the liquid-solid interface. *Top. Curr. Chem.* **287**, 87–133 (2009).
- Lei, S. B., Tahara, K., Adisojoso, J., Tobe, Y. & De Feyter, S. Towards two-dimensional nanoporous networks: crystal engineering at the solid-liquid interface. *CrystEngComm*. **12**, 3369–3381 (2010).

- Elemans, J. A. A. W., Lei, S. B. & De Feyter, S. Molecular and supramolecular networks on surfaces: from two-dimensional crystal engineering to reactivity. *Angew. Chem., Int. Ed.* **48**, 7298–7332 (2009).
- Furukawa, S. *et al.* Molecular geometry directed kagomé and honeycomb networks: towards two-dimensional crystal engineering. *J. Am. Chem. Soc.* **128**, 3502–3503 (2006).
- Henningsen, N. *et al.* Site-dependent coordination bonding in self-assembled metal-organic networks. *J. Phys. Chem. Lett.* **2**, 55–61 (2011).
- Gambardella, P. *et al.* Supramolecular control of the magnetic anisotropy in two-dimensional high-spin Fe arrays at a metal interface. *Nat. Mater.* **8**, 189–193 (2009).
- Loew, G. H. & Harris, D. L. Role of the heme active site and protein environment in structure, spectra, and function of the cytochrome P450s. *Chem. Rev.* **100**, 407–420 (2000).
- Kley, C. S. *et al.* Highly adaptable two-dimensional metal-organic coordination networks on metal surfaces. *J. Am. Chem. Soc.* **134**, 6072–6075 (2012).
- Fabris, S. *et al.* Oxygen dissociation by concerted action of di-iron centers in metal-organic coordination networks at surfaces: modeling non-heme iron enzymes. *Nano Lett.* **11**, 5414–5420 (2011).
- Palma, C. A., Bonini, M., Breiner, T. & Samori, P. Supramolecular crystal engineering at the solid-liquid interface from first principles: toward unraveling the thermodynamics of 2D self-assembly. *Adv. Mater.* **21**, 1383–1386 (2009).
- Kikkawa, Y. *et al.* Odd-even effect and metal induced structural convergence in self-assembled monolayers of bipyridine derivatives. *Chem. Commun.* 1343–1345 (2007).
- Shubina, T. E. *et al.* Principle and mechanism of direct porphyrin metalation: joint experimental and theoretical investigation. *J. Am. Chem. Soc.* **129**, 9476–9483 (2007).
- Li, Y. *et al.* Coordination and metalation bifunctionality of Cu with 5,10,15,20-Tetra(4-pyridyl)porphyrin: toward a mixed-valence two-dimensional coordination network. *J. Am. Chem. Soc.* **134**, 6401–6408 (2012).
- Li, Y. & Lin, N. Combined scanning tunneling microscopy and kinetic Monte Carlo study on kinetics of Cu-coordinated pyridyl-porphyrin supramolecular self-assembly on a Au(111) surface. *Phys. Rev. B* **84**, 125418–125424 (2011).
- Visser, J., Katsonis, N., Vicario, J. & Feringa, B. L. Two-dimensional molecular patterning by surface-enhanced zn-porphyrin coordination. *Langmuir* **25**, 5980–5985 (2009).
- Liu, J. *et al.* Structural transformation of two-dimensional metal-organic coordination networks driven by intrinsic in-plane compression. *J. Am. Chem. Soc.* **133**, 18760–18766 (2011).
- Langer, A. *et al.* Selective coordination bonding in metallo-supramolecular systems on surfaces. *Angew. Chem. Int. Ed.* **51**, 4327–4331 (2012).
- Lu, J. *et al.* Template-induced inclusion structures with copper (II) phthalocyanine and coronene as guests in two-dimensional hydrogen-bonded host networks. *J. Phys. Chem. B* **108**, 5161–5165 (2004).
- Shen, Y. T., Guan, L., Zhu, X. Y., Zeng, Q. D. & Wang, C. Submolecular observation of photosensitive macrocycles and their isomerization effects on host-guest network. *J. Am. Chem. Soc.* **131**, 6174–6180 (2009).
- Shen, Y. T. *et al.* Switchable ternary nanoporous supramolecular network on photo-regulation. *Nano Lett.* **11**, 3245–3250 (2011).
- Shen, Y. T., Deng, K., Zeng, Q. D. & Wang, C. Size-selective effects on fullerene adsorption by nanoporous molecular networks. *Small* **6**, 76–80 (2010).
- Liu, J. *et al.* Chiral hierarchical molecular nanostructures on two-dimensional surface by controllable trinary self-assembly. *J. Am. Chem. Soc.* **133**, 21010–21015 (2011).
- Ciesielski, A., Lena, S., Masiero, S., Spada, G. P. & Samor, P. Dynamers at the solid-liquid interface: controlling the reversible assembly/reassembly process between two highly ordered supramolecular guanine motifs. *Angew. Chem. Int. Ed.* **49**, 1963–1966 (2010).
- Zeng, Q. D. *et al.* Bipyridine conformations control the solid-state supramolecular chemistry of zinc(II) phthalocyanine with bipyridines. *CrystEngComm*. **7**, 243–248 (2005).
- Delley, B. J. From molecules to solids with the DMol3 approach. *Chem. Phys.* **113**, 7756–7764 (2000).
- Delley, B. An all-electron numerical method for solving the local density functional for polyatomic molecules. *J. Chem. Phys.* **92**, 508–517 (1990).
- Becke, A. D. A multicenter numerical integration scheme for polyatomic molecules. *J. Chem. Phys.* **88**, 2547–2553 (1988).
- Perdew, J. P. & Wang, Y. Accurate and simple analytic representation of the electron-gas correlation energy. *Phys. Rev. B* **45**, 13244–13249 (1992).

Acknowledgements

This work was supported by the National Basic Research Program of China (No. 2011CB932303, 2012CB933001). Financial supports from the National Natural Science Foundation of China (Nos. 21073048, 51173031, 91127043, 20933008) are also gratefully acknowledged.

Author contributions

Q.-D. Z. and C. W. contributed to the conception and design of the experiments, analysis of the data and revising the paper. K. D. finished the DFT calculation. S. W. carried out the



synthetic experiments. Y.-T. S. constructed the molecular models. Y.-Y. G. optimized the experimental parameters. X.-M. Z. designed and carried out the STM experiments, analyzed the data and wrote the paper.

Additional information

Supplementary information accompanies this paper at <http://www.nature.com/scientificreports>

Competing financial interests: The authors declare no competing financial interests.

License: This work is licensed under a Creative Commons Attribution-NonCommercial-NoDerivative Works 3.0 Unported License. To view a copy of this license, visit <http://creativecommons.org/licenses/by-nc-nd/3.0/>

How to cite this article: Zhang, X. *et al.* One plus Two: Supramolecular Coordination in a Nano-Reactor on Surface. *Sci. Rep.* 2, 742; DOI:10.1038/srep00742 (2012).